

A.A. Bulychev · S.V. Zykov · A.B. Rubin · S.C. Müller

## Transitions from alkaline spots to regular bands during pH pattern formation at the plasmalemma of *Chara* cells

Received: 1 July 2002 / Revised: 12 December 2002 / Accepted: 13 December 2002 / Published online: 6 March 2003  
© EBSA 2003

**Abstract** A scanning pH-microprobe was used to study pH patterns near the surface of *Chara corallina* cells at various light intensities and during light-induced transitions from homogeneous pH distribution to alternating pH bands. In the irradiance (PAR) range 4–400  $\mu\text{mol quanta m}^{-2} \text{s}^{-1}$ , the sustained pH profiles consisted of alternating acid and alkaline bands with a characteristic length of 7–10 mm and pH shifts as large as 2–3 units. At lower irradiances, the number of alkaline bands decreased while the amplitude of remaining peaks stayed high. On cyclic changes in light intensity, a hysteresis of pH banding was observed: the pH bands tolerated low irradiance in weakening light, but higher irradiance was required for their emergence after dark adaptation of the cell. The pH profiles measured for different paths of electrode scanning suggest that the pH pattern at low light level represents patches coexisting with bands. The exposure of the cell to high-intensity light led to formation of radially symmetrical bands. Transformations of the pH pattern induced by lowering the light intensity were similar to those induced by transcellular electric current (1.5–3  $\mu\text{A}$ ). The data suggest that band formation at the plasmalemma of *Chara* cells proceeds through the initial appearance of multiple patches with a localized  $\text{H}^+$ -transporting activity and subsequent spot rearrangements (fusion, deletions, widening), leading to establishment of alternating bands.

**Keywords** Alkaline and acid bands · *Chara corallina* Hysteresis · pH microelectrode · Photosynthesis

S.V. Zykov · S.C. Müller (✉)  
Institut für Experimentelle Physik,  
Otto-von-Guericke Universität,  
Universitätsplatz 2, 39106 Magdeburg, Germany  
E-mail: stefan.mueller@physik.uni-magdeburg.de  
Tel.: +49-391-6718338  
Fax: +49-391-6711181

A.A. Bulychev · S.V. Zykov · A.B. Rubin  
Biophysics Department, Faculty of Biology,  
Moscow State University, 119899 Moscow, Russia

### Introduction

Characean cells (*Chara*, *Nitella*, *Nitelopsis*), when exposed to light, develop alternating acid and alkaline zones on their surface (Spear et al. 1969; Walker and Smith 1977; Lucas and Nucitelli 1980; Lucas et al. 1983; Fisahn and Lucas 1991). This light-dependent phenomenon is thought to result from the inhomogeneous distribution of proton pump and proton sink activities over the plasma membrane (Walker and Smith 1977; Toko et al. 1985, 1988; Fisahn et al. 1992). The ATP-fuelled proton pumps extrude protons from the cytoplasm, creating acid zones near the cell surface, whereas the massive influx of protons occurs in the alkaline regions and is presumably mediated by the high pH channels (Bisson and Walker 1980; Beilby et al. 1993). The concerted operation of pumps and sinks generates local circulating currents flowing in the external medium from the acid areas to alkaline regions (Walker and Smith 1977). These currents can be detected with a vibrating electrode technique as a suitable indicator of acid and alkaline areas (Lucas et al. 1983). The banding pattern is not solely confined to the plasmalemma but manifests itself also in spatially heterogeneous photosynthetic activity of chloroplasts in different cell zones (Bulychev et al. 2001a).

The banding phenomena were mostly investigated under light sufficiency, when the pattern is best developed. Much less is known on how these phenomena depend on light intensity, particularly at low light, when the pH pattern is about to vanish. Lucas (1975) reported that the pH pattern arises in continuous light if the light intensity is above a certain threshold level. He also found that the formation of alkaline bands following the transfer of a dark-adapted cell to light occurs after a lag period, the duration of which shortens when the light intensity is increased. The dynamics of the pH patterns in the critical range is of particular interest for understanding their origin. It is not known whether the number and position of the

bands remains constant during pattern formation or if it is subject to substantial changes. However, discontinuous point-by-point pH measurements, employed in earlier studies (Lucas 1975; Lucas and Nuccitelli 1980), are insufficient for adequate spatial and temporal resolution of primary events in the transition from a homogeneous state to the banding pattern. The vibration probe technique provides better spatial resolution of extracellular currents, but rigorous mixing may perturb ion profiles in the boundary layers (Lucas and Nuccitelli 1980). As far as we know, this technique was not employed for studying circulating currents at variable light intensities, but only contrasting light conditions, such as bright light and darkness, were applied (Lucas and Ogata 1985; Fisahn and Lucas 1990). Interestingly, there were diverse reports on the location of extracellular current bands after temporary darkening and reillumination. In experiments on *Chara* cells, the bands reappeared at the same locations as before darkening (Frost-Shartzner et al. 1992). Nevertheless, Fisahn and Lucas (1990) observed a population of *Nitella* cells showing the inversion of banding profiles after reillumination.

Recently, a scanning pH-microprobe technique was introduced for recording continuous pH profiles along the surface of internodal *Chara* cells (Bulychev et al. 2001a, 2001b). The non-invasive scanning with a pH microprobe allows long-lasting measurements of pH profiles with a sufficient temporal and spatial resolution. With this direct method it was shown that nearly 100-fold variation in light intensity has only a slight effect on the banding pattern, whereas further decrease in the light intensity results in the disappearance of alkaline and acid bands. However, the transformations of the banding profile in the critical range of light intensities have not yet been analyzed.

The measurements of pH profiles for different pathways along the same cell have revealed that alkaline zones may occur as local patches or band extensions, coexisting with regular closed bands (Bulychev et al. 2001b). Such data on pH profiles along parallel pathways, shifted along the cell perimeter, can be used to distinguish the band- and patch-like pH patterns near the cell surface. This approach seems promising for studying the evolution of a pH pattern while it emerges from the uniform distribution.

The goal of this work was to investigate the appearance and evolution of the pH pattern at low light intensities, when the transition between a homogeneous state and banding structures takes place. Such a study is essential for understanding the origin of pH banding as a manifestation of self-organization on the single-cell level. In order to find out whether the heterogeneous pH distribution at early stages of pattern formation correlates with the structures sustained at high illumination, we compare the longitudinal pH profiles that were obtained for pH-microprobe scans shifted along the cell perimeter. We find that the transition from the homogeneous state towards banding structures in low light

occurs via temporary patch-like patterns consisting of alkaline spots.

## Materials and methods

*Chara corallina* Klein ex Willd. was grown in glass vessels under scattered daylight at room temperature (20–22 °C). Internodal cells measuring 6–7 cm in length and about 1 mm in diameter were cut from the plant and placed in artificial pond water containing 0.1 mM KCl, 1.0 mM NaCl and 0.1 mM CaCl<sub>2</sub>. Experiments were performed on cells with scarce calcium depositions visible under the microscope. Prior to an experiment, the cell was fixed in a Plexiglas chamber, which was mounted on a movable table controlled by a C-804 DC motor controller (Physik Instrumente, Waldbronn, Germany).

The cell was illuminated from underneath with white light provided from a 250 S-AF projector (Braun Photo Technik). The light beam was directed upward with a plane mirror and reached the cell through the transparent bottom of the experimental chamber. The maximum irradiance at the cell level was 430  $\mu\text{mol quanta m}^{-2} \text{s}^{-1}$  and was attenuated with a set of NG 9 and NG 11 neutral density glass filters placed in proximity to the projector lens. Light intensities were measured with a J17 TEK Lumacolor Photometer (Tektronix). The photometer readings of irradiance ( $\text{W m}^{-2}$ ) were recalibrated to photosynthetic quantum flux densities (the radiant energy between 400 and 700 nm). This was accomplished by measuring the spectral distribution of the energy of actinic light in the visible and near infrared (< 850 nm) range at 1 nm intervals.

The longitudinal pH profiles near the cell surface were measured with tip-sensitive pH microelectrodes. These were pulled on a vertical puller from Pyrex capillaries (1.2 mm outer diameter) filled with melted antimony. The tip diameter of the microelectrodes varied from 10 to 50  $\mu\text{m}$ . The potential difference between the pH probe and Ag/AgCl reference electrode was graduated as a function of pH using standard buffer solutions. The slope of the electrode response was 56 mV/pH unit. The potential difference was measured with a VAJ-51 high-impedance ( $10^{15} \Omega$ ) electrometric amplifier, digitized, and recorded on a computer.

The pH microprobe was mounted in a microelectrode holder and positioned with a micromanipulator. Prior to each measurement, the pH microelectrode was placed near one end of the internode. Then, the cell was moved along its axis at a constant velocity of 200  $\mu\text{m s}^{-1}$  relative to the immobile pH probe over a length up to 50 mm. During the scanning, the distance between electrode tip and cell wall was kept at 20–50  $\mu\text{m}$  and was slightly readjusted when the cell was not perfectly straight. In some experiments the position of the pH microprobe was shifted along the cell perimeter after each individual measurement. This way, up to nine parallel pH scans with a peripheral distance  $\geq 200 \mu\text{m}$  could be measured.

At the beginning of each experiment, the capacity of the cell to form pH bands was checked at high light intensity. Next, the light intensity was either reduced or the cell was placed in darkness to eliminate acid and alkaline bands. When a homogenous distribution of pH was attained within 1–2 h, the cell was exposed to a graded series of light intensities. At each level of light intensity, pH profiles were measured at intervals of 10 min for at least 40 min until reproducible records were obtained.

In experiments involving transcellular current, the cell was placed in a three-sectioned chamber (see Fig. 7a). The nodes with adjoining cell regions were placed in peripheral compartments, and the central part of the internode occupied the middle compartment. The solutions in the central and side compartment were electrically insulated with silicone grease gaps (Baysilone paste, GE Bayer Silicones). The pH profile measurements were performed on the central cell part in the middle compartment, where the reference electrode was also placed. The silver-wire electrodes for passing current were fixed in the side compartments and connected to an NTL05 DC power supply (PTM Elektronik) via a 10 M $\Omega$  load

resistor. The current strength was measured from the voltage drop across this resistor. The connection of electrodes to the current circuit and the passage of transcellular current had no immediate effect on the potential difference in the measuring circuit (i.e., on pH readings).

The pH profiles shown in the following section are representative records out of 3–5 replicate measurements. Under steady-state conditions, replicate measurements yielded similar pH profiles with reproducible fine structure. The plots of the pH shift between adjacent acid and alkaline zones ( $\Delta\text{pH}$ ) as a function of increasing and decreasing light intensity were obtained from data of seven experiments on different cells after normalizing the  $\Delta\text{pH}$  values. Each point on these plots represents a  $\Delta\text{pH}$  value recorded about 40 min after the transfer of the cell to the given light intensity.

## Results

### Number of bands at various light intensities

Figure 1 exemplifies the steady-state pH profiles at various light intensities, when the experiment was started from the homogenous state of a dark-adapted cell. At light intensities below  $0.4 \mu\text{mol quanta m}^{-2} \text{s}^{-1}$ , the pH profiles were completely flat. The first waves in the smooth pH profile were observed after a stepwise increase of irradiance to  $1 \mu\text{mol quanta m}^{-2} \text{s}^{-1}$ . Under constant light conditions, one of these waves suddenly

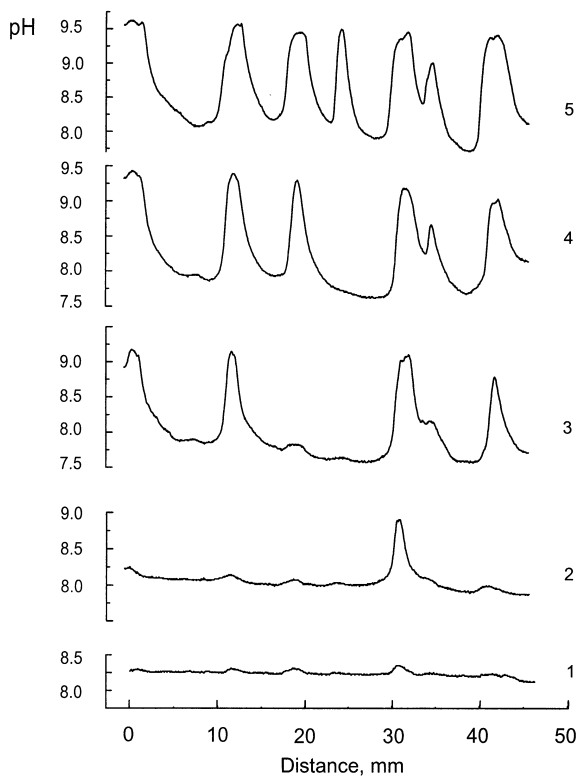


**Fig. 1** Formation of longitudinal pH profiles in *Chara* cell upon a stepwise increase in light intensity. (1) pH profile measured 20 min after increase in light intensity from  $0.4 \mu\text{mol quanta m}^{-2} \text{s}^{-1}$  to  $1.0 \mu\text{mol m}^{-2} \text{s}^{-1}$ ; (2) after 60 min exposure at  $1.0 \mu\text{mol quanta m}^{-2} \text{s}^{-1}$ ; (3) steady-state pH profile at  $7.7 \mu\text{mol quanta m}^{-2} \text{s}^{-1}$ ; (4)  $16.3 \mu\text{mol m}^{-2} \text{s}^{-1}$ ; (5)  $430 \mu\text{mol m}^{-2} \text{s}^{-1}$ .

evolved into a sharp peak, giving rise to a stable one-peak profile with a pH change of 0.8 pH units (compare curves 1 and 2). The subsequent increase of this peak, when further elevating the light intensity, occurred in a gradual manner, not as steep as the initial rise. A step-by-step increase in light intensity over a wide intensity range increased the number of bands up to seven (curves 2–5). Many of these bands were formed at the same locations where the initial waves were noticed. Similar alterations of longitudinal pH profiles were observed on other cells, although the location and number of bands varied for different internodes. Under high light conditions, the external pH along the surface of a *Chara* cell is subject to spatial variations with a characteristic length scale of 5–10 mm, and pH differences between acid and alkaline zones as high as 3 pH units are observed.

Figure 2 shows an experiment in which the light intensity was decreased in a stepwise manner. The reduction from  $430 \mu\text{mol quanta m}^{-2} \text{s}^{-1}$  to about  $5 \mu\text{mol quanta m}^{-2} \text{s}^{-1}$  had only a slight effect on the number and amplitude of alkaline bands (not shown). Below  $2 \mu\text{mol m}^{-2} \text{s}^{-1}$ , some bands were eliminated, whereas the remaining bands were only slightly reduced in their amplitude. The pattern with a reduced number of bands was stable at a given light intensity and could be reproduced in sequential measurements for several hours. Upon further attenuation of light, more bands disappeared from the pH profile (see profile 1–3 in Fig. 2). At low light ( $0.02$ – $1 \mu\text{mol m}^{-2} \text{s}^{-1}$  for various cells), pH profiles with only one or two sharp peaks were observed. When the last sharp peaks disappeared, low-amplitude undulations (0.1–0.3 pH) were seen. Complete smoothing of the pH profile required 40–120 min of darkness, depending on the cell.

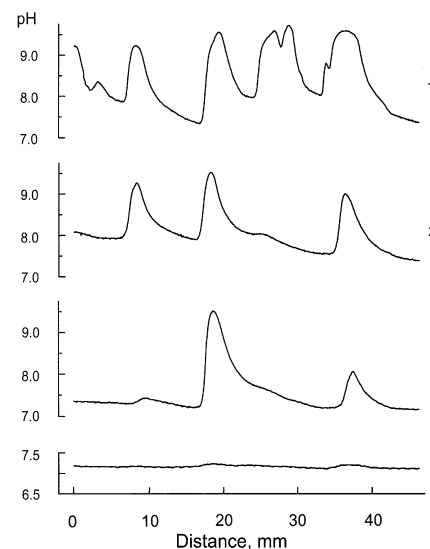


**Fig. 2** Changes of steady-state pH profiles upon a stepwise reduction in light intensity. (1) pH profile at  $430 \mu\text{mol quanta m}^{-2} \text{s}^{-1}$ ; (2)  $0.37 \mu\text{mol m}^{-2} \text{s}^{-1}$ ; (3)  $0.033 \mu\text{mol m}^{-2} \text{s}^{-1}$ ; (4) after 100 min in darkness. Records were obtained after 40-min exposure of the cell to a given light intensity

In Fig. 3a the amplitude (curve 1) and the number of bands (curve 2) are shown in one of the experiments as a function of decreasing light intensity. The amplitude was measured as the largest pH difference between neighboring acid and alkaline zones. The number of alkaline peaks decreased markedly in a range where the amplitude of the pH shift remained constant. Thus, over a wide range, the changes in light intensity affect primarily the number of pH peaks and exert comparatively weak action on their amplitude. It is also noteworthy that the last alkaline peak was more resistant to a decreasing level of illumination than the other peaks; the intensity range of its existence was much wider as compared to other alkaline bands.

### Hysteresis of light-intensity curves

Figures 1 and 2 suggest that, upon decreasing irradiance, the last band (Fig. 2, curve 3) persisted at a light intensity much lower than that required for the generation of the first band in increasing light (Fig. 1, curve 2). The plots of  $\Delta\text{pH}$  as a function of descending and increasing irradiances (Fig. 3a, curve 1, and Fig. 3b) deviated markedly. The rise of  $\Delta\text{pH}$  upon the increase in light intensity occurred at comparatively high intensities (light attenuation factor  $\sim 10^3$ ) for all the cells examined. Figure 3b shows such a plot for one individual cell. The number of bands is not shown, as it was not a clearly defined parameter when small peaks of variable magnitude were present during band formation at increasing light intensities. As shown in a previous study, the break of homogeneous pH distribution after a stepwise increase in light intensity proceeds through formation of small alkaline peaks, some of which disappear upon the transition to a steady state (Bulychev et al. 2001b).

Figure 3c summarizes the data obtained from seven cells. For comparison, the  $\Delta\text{pH}$  values were normalized to the average  $\Delta\text{pH}$  at light intensities  $\geq 4 \mu\text{mol m}^{-2} \text{s}^{-1}$ . It is seen that, in decreasing light, the  $\Delta\text{pH}$  between alkaline and acid regions remained high (with a few exceptions) when light was attenuated to ca.  $0.05 \mu\text{mol quanta m}^{-2} \text{s}^{-1}$  (attenuation factor  $\sim 10^4$ ). Conversely, no appreciable  $\Delta\text{pH}$  was ever observed at this light level upon a gradual increase in light intensity. Thus, Fig. 3a–c provides evidence for hysteresis in the pH response upon cyclic reduction and elevation of light intensity.

### Two stable states for pH distribution at equal light intensities

Bistable behavior as a consequence of the hysteretic properties of alkaline band formation was verified in the following way. Depending on the preconditioning of a *Chara* cell, either flat or banding pH profiles were recorded at equal light intensity. In these experiments, the cell was exposed to two cycles of increasing and

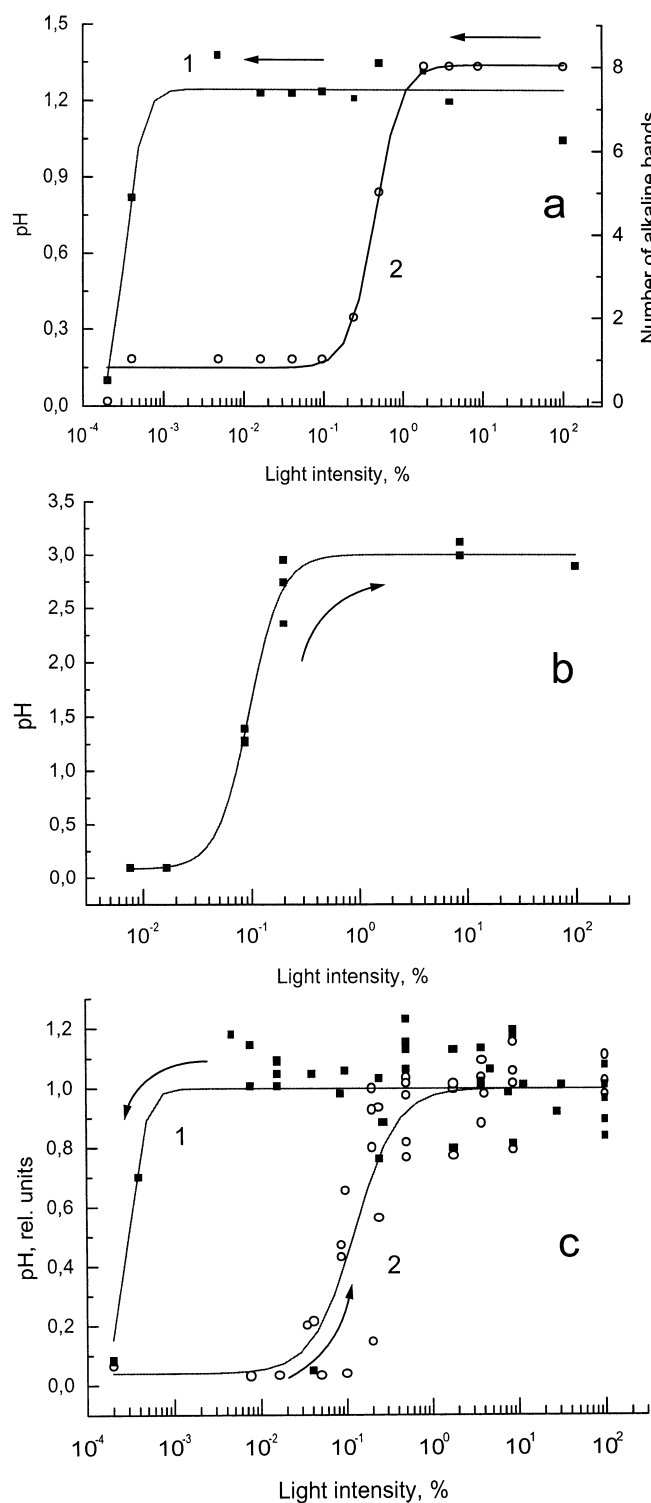


**Fig. 3** Effects of decreasing and increasing light intensity on pH banding pattern along *Chara* cells. (a)  $\Delta\text{pH}$  in an individual cell (the pH difference between neighboring alkaline and acid zones, squares, curve 1) and the number of alkaline bands (circles, curve 2) as a function of decreasing light intensity, starting from  $430 \mu\text{mol quanta m}^{-2} \text{s}^{-1}$  (100%); (b)  $\Delta\text{pH}$  in an individual cell as a function of increasing light intensity; (c) normalized  $\Delta\text{pH}$  as a function of decreasing (filled squares) and increasing light intensity (open circles). Average  $\Delta\text{pH}$  values obtained on various cells at irradiance range  $4.3\text{--}430 \mu\text{mol m}^{-2} \text{s}^{-1}$  were normalized to a value of 1.0

decreasing incident light. When the cell was transferred from darkness to irradiances of 1.0 and then  $2.2 \mu\text{mol quanta m}^{-2} \text{s}^{-1}$ , the pH profile remained flat for at least 30 min at each light level. A transition to a higher light level ( $7.7 \mu\text{mol m}^{-2} \text{s}^{-1}$ ) led within 20 min to band formation. On subsequent reduction of quantum flux density to  $2.2 \mu\text{mol m}^{-2} \text{s}^{-1}$ , the alkaline bands remained unaltered within at least 30 min. The existence of two stable states at the same light level was reproduced in the second cycle of corresponding light intensity changes.

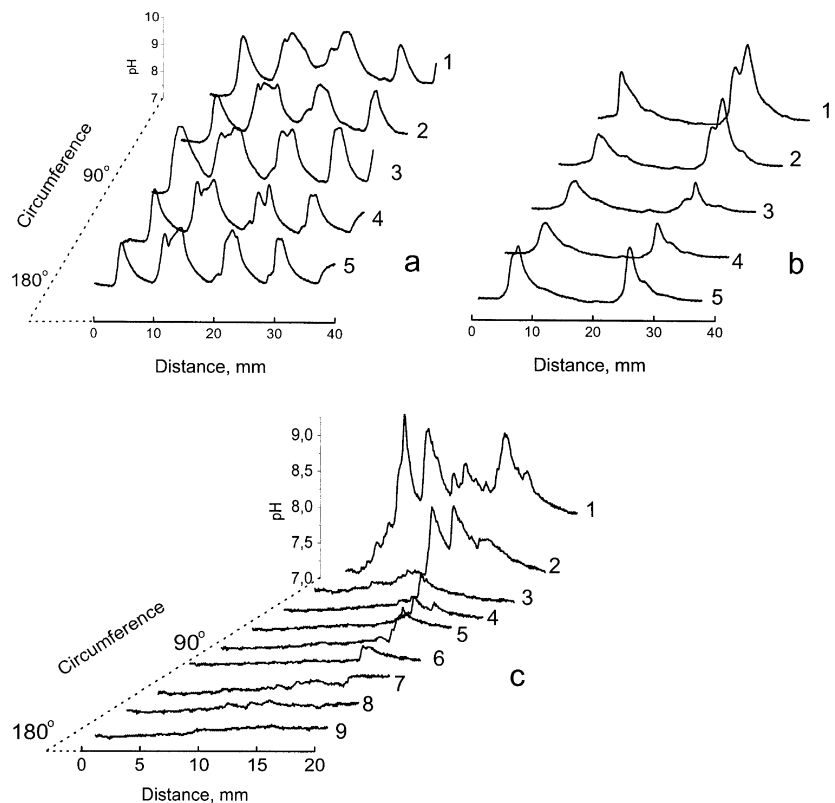
#### Patches and bands as elements of the pH pattern near the cell surface

The cell-surface pH profiles were measured by scanning with the pH microprobe along several parallel pathways shifted along the cell perimeter. Such measurements on various cells revealed substantial differences in the spatial distribution of the external pH near the *Chara* cell. Structures of two types, bands and spots, were distinguished. Figure 4 illustrates the difference between these structures. In an experiment shown in Fig. 4a and Fig. 4b, the scanning pH measurements were performed along five evenly spaced tracks in the upper half of the cell. All five records showed similar alternating alkaline peaks, indicating that alkaline areas can be attributed to bands. Strictly speaking, these bands are at least "half closed." There were more

bands at high ( $430 \mu\text{mol quanta m}^{-2} \text{s}^{-1}$ ) than at moderate ( $2.2 \mu\text{mol m}^{-2} \text{s}^{-1}$ ) irradiance (Fig. 4a and Fig. 4b, respectively). In the latter case, the alkaline peaks were not uniform in magnitude: the pH peaks measured near the upper side (trace 3) were smaller than those measured on opposite lateral sides of the cell (traces 1, 5).

The pH profiles shown in Fig. 4c were obtained on another cell at an irradiance of  $80 \mu\text{mol quanta m}^{-2} \text{s}^{-1}$ . This cell (from another batch of algae) differed in appearance by a deeper green color, which is indicative of higher chlorophyll content. Measurements were conducted along nine neighboring paths. In this case, scanning the electrode near one lateral side (trace 1) produced a pH profile with several peaks amounting to 1.5–2.0 pH units. Scanning the electrode along the next parallel path (trace 2) yielded a profile in which some peaks were suppressed and others shifted. For distant electrode paths (traces 7–9), the pH profiles were almost flat. The differences between the traces were seen in a repetitive set of measurements, which excludes temporal changes during the experiment. Obviously, the pH profile in trace 1 represents local pH changes that do not extend over the cell perimeter and thus correspond to spots (patches) on the cell surface. The comparison of pH profiles similar to curve 1 for replicate data sets revealed differences in their fine structure (data not shown). These differences might reflect the existence of highly dispersed domains with  $\text{H}^+$  sink activities, confined to restricted areas on the

**Fig. 4** Examples of pH banding pattern (a, b) and spots (c) in different *Chara* cells. (a) Series of pH profiles recorded at equidistantly spaced paths in the upper half of the internodal cell at a light intensity of  $430 \mu\text{mol quanta m}^{-2} \text{s}^{-1}$ ; (b) pH profiles in the same cell at  $2.2 \mu\text{mol quanta m}^{-2} \text{s}^{-1}$ ; (c) pH profiles recorded in the upper half of a different cell at a light intensity of  $80 \mu\text{mol quanta m}^{-2} \text{s}^{-1}$ . The inhomogeneous angular pH distribution in (c) on one cell side represents local spots rather than bands



cell surface, or temporal fluctuations of pH in these local regions.

Thus, at high light levels, the pH pattern may consist of either bands or local spots (patches). This observation raises the question whether the pattern type is invariant from the onset of formation or, alternatively, the contribution of bands and patches changes during the pattern evolution under different light intensities. The possibility of such an interplay between patches and bands was considered in the experiments below.

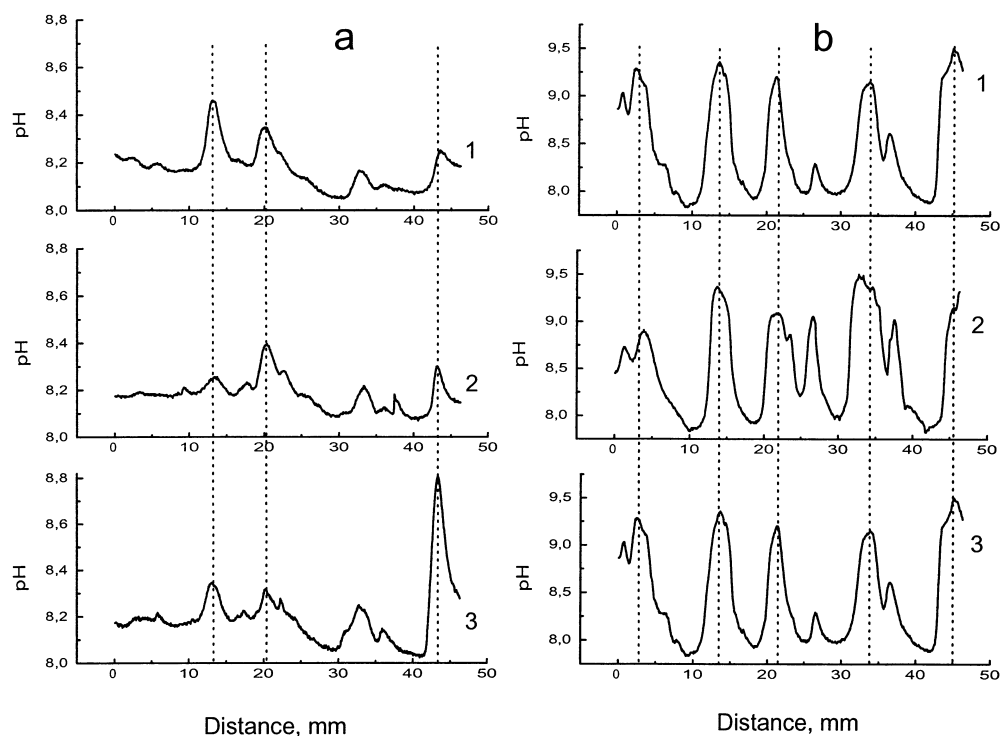
#### Rearrangement of patch to band pattern upon the transition from low to high light intensity

In these experiments, we routinely measured the profiles for two paths on opposite sides of the cell or three paths shifted by  $90^\circ$  in angular coordinates. In many cases, this procedure already sufficed to distinguish the band and spot patterns and was less time-consuming than serial measurements along multiple pathways. When measured at reduced light intensities, the pH profiles along different paths consisted of small narrow peaks variable in amplitude and position. Figure 5a shows the traces obtained for three paths at an irradiance of  $2.2 \mu\text{mol m}^{-2} \text{s}^{-1}$ . Measurements along the three paths were made in sequence, and such sets of sequential measurements were repeated four times. The pH profiles obtained within 2–3 h showed slight temporal variations, indicating that steady-state conditions were not attained. Nevertheless, these profiles were fairly reproducible for each lane and showed marked distinctions for different lanes. For example, the alkaline peak positioned near 43 mm was

several times larger for path 3 than for other ones. These path-dependent distinctions indicate that small peaks represented alkaline patches on the cell surface rather than uniform ring-shaped structures. When the same cell was exposed to increasing light intensities, the pH profiles for various paths showed common peaks. In high light, the profiles measured for all three paths were similar, indicating the formation of band structures (Fig. 5b).

Figure 6 provides evidence that during the evolution of a pH pattern some patches appear as temporary structures and are eliminated in the steady-state profiles. It shows the pH profiles measured for two electrode pathways at a moderate light intensity of  $2.2 \mu\text{mol quanta m}^{-2} \text{s}^{-1}$  under steady-state conditions (curves 1 and 3) and in the period of band formation (curves 2 and 4). When the cell was illuminated for 2 h in the beginning of the experiment, the pH profiles on the opposite cell sides were similar, containing one main peak (curves 1). This similarity allows the assignment of the peaks to a band. Then, the cell was kept for 3 h in darkness, and the pH profiles were smoothed out (not shown). Forty minutes after transferring the dark-adapted cell to light of the same intensity, the pH profiles were strikingly different (compare curves 2 for paths 1 and 2), with peaks located at different positions (near 30 and 40 mm, respectively), indicating their attribution to alkaline spots. After prolonged light exposure (2.5 h), the main peaks occupied their initial locations (curves 3), indicating that the spot–band transition was accomplished. The experiment was repeated by placing the cell in darkness for 2 h to establish the homogenous state and by subsequent illumination to induce the pH pattern. In

**Fig. 5** Transformation of patchy pattern (a) observed at low ( $2.2 \mu\text{mol quanta m}^{-2} \text{s}^{-1}$ ) to band pattern (b) at higher light intensities ( $38 \mu\text{mol quanta m}^{-2} \text{s}^{-1}$ ). Traces 1 and 3 are pH profiles at opposite lateral sides of the cell (rear and front sides, respectively); trace 2 is the pH profile near the upper side of the cell. Nonuniform peaks in traces in (a) represent alkaline spots, whereas uniform peaks for all traces in (b) represent alkaline bands



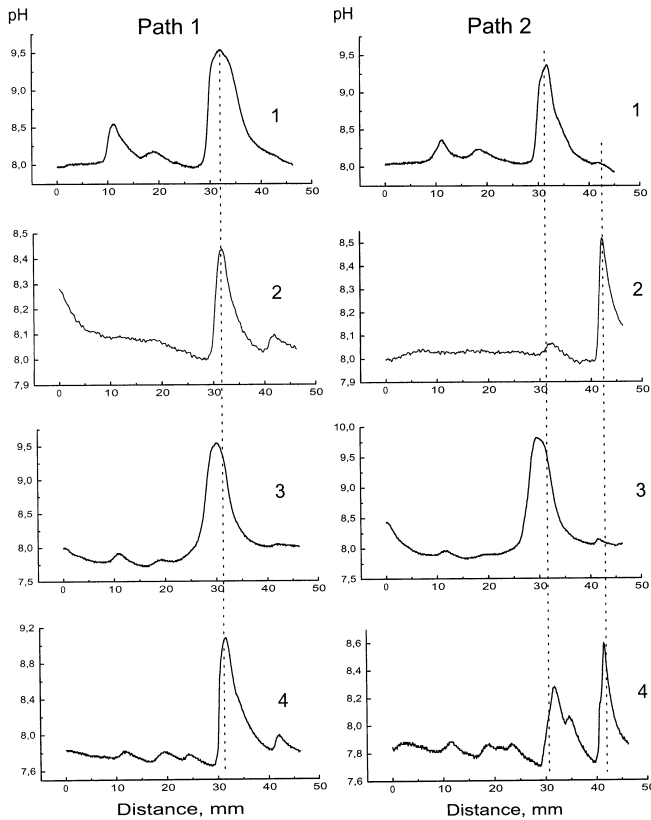


**Fig. 6** Changes in the pH patterns on *Chara* cells during the transition to the steady state. *Left and right columns (paths 1 and 2)* represent pH profiles measured along different pathways on opposite sides of the cell. Similarities in these profiles indicate a band pattern (*curves 1, 3*), whereas differences in position and amplitude of peaks is evidence of patch structures (*curves 2, 4*). Profiles 1–4 were measured sequentially under the following conditions: 1, cell illuminated for 1 h at  $2.2 \mu\text{mol quanta m}^{-2} \text{s}^{-1}$ ; 2, cell kept in darkness for 3 h and then exposed to light ( $2.2 \mu\text{mol m}^{-2} \text{s}^{-1}$ ) for 40 min; 3, cell kept at  $2.2 \mu\text{mol m}^{-2} \text{s}^{-1}$  for 2.5 h; 4, cell kept in darkness for 2 h and then exposed to light ( $2.2 \mu\text{mol m}^{-2} \text{s}^{-1}$ ) for 50 min. The profiles 1 and 3 represent the steady state, and profiles 2 and 4 are transient structures occurring during the transition to the steady state

this pattern, the alkaline peak at a location of  $\sim 40$  mm was restored in path 2 but it was missing in path 1 (curves 4). The data suggest that this peak represents an alkaline spot that appeared transiently at the initial stages of pattern formation and was eliminated while the transition to a regular band structure took place.

#### Effect of transcellular electric current on alkaline bands

The origin of acid and alkaline bands is closely related to electric currents flowing from acid to alkaline regions in the outer medium and in the opposite direction into the cell interior (Walker and Smith 1977; Fisahn and Lucas 1990). We attempted to disturb these local currents by letting an electric current pass longitudinally through the internode, as shown in the diagram of Fig. 7a (see also

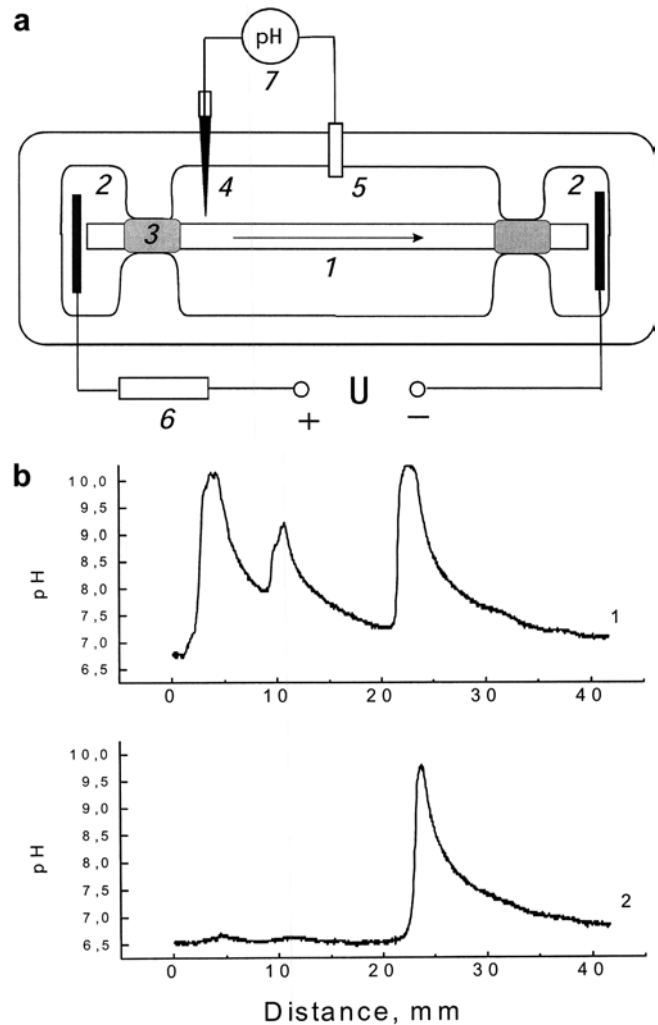


**Fig. 7** Effect of transcellular current on longitudinal pH profiles in illuminated *Chara* cell. (a) Experimental setup for passing current through the *Chara* internode: 1, internodal cell; 2, Ag wire electrodes for passing current; 3, insulating gaps (Baysilone grease); 4, pH microelectrode; 5, reference Ag/AgCl electrode; 6, load resistor ( $10 \text{ M}\Omega$ ) used for stabilizing the current; 7, electrometer. Arrow indicates the direction of transcellular current. (b) Modification of pH profiles by the transcellular current: 1, pH profile under control conditions (white light,  $430 \mu\text{mol quanta m}^{-2} \text{s}^{-1}$ ); 2, pH profile in the same cell under identical light conditions after passing a transcellular electric current ( $1.7 \mu\text{A}$ ) for 10 min

Materials and methods). This superposition would elevate the current density in cell regions where local and imposed currents have coincident directions, and would diminish it in regions where their directions are opposite. According to Fig. 7b, the transcellular current flow ( $1.7 \mu\text{A}$ , 10 min) eliminated some bands in the longitudinal pH profile without affecting the amplitude of the remaining bands. Such current-induced modification of the banding pattern is reminiscent of that induced by exposure to low light levels.

This similarity is further illustrated in Fig. 8, which shows that a reduction in light intensity caused disappearance of the third and fifth large bands in the profile that consisted of seven alkaline bands (cf. Fig. 8a and

**Fig. 8** Elimination of some alkaline bands in the longitudinal pH profile by the exposure of illuminated *Chara* cell (irradiance  $430 \mu\text{mol quanta m}^{-2} \text{s}^{-1}$ ) to low light intensity ( $1.0 \mu\text{mol m}^{-2} \text{s}^{-1}$ ) or transcellular current ( $1.7 \mu\text{A}$ ): (a) control conditions,  $430 \mu\text{mol quanta m}^{-2} \text{s}^{-1}$ ; (b) low light intensity,  $1.0 \mu\text{mol quanta m}^{-2} \text{s}^{-1}$ ; (c) after passing current ( $1.7 \mu\text{A}$ , 10 min) at control light; (d) after passing current ( $1 \mu\text{A}$ , 20 min) at low light intensity

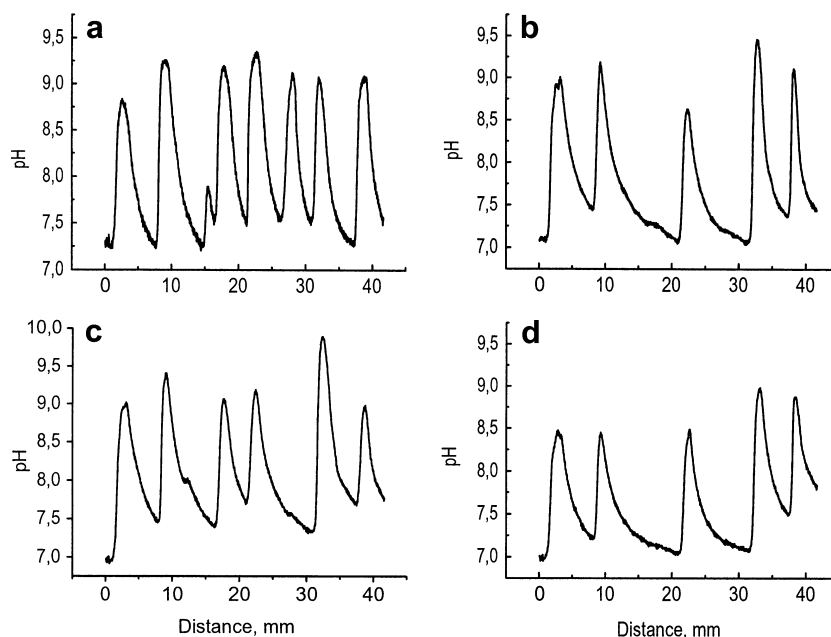


Fig. 8b). The initial pH pattern was restored under high light conditions ( $200 \mu\text{mol quanta m}^{-2} \text{s}^{-1}$ ) (not shown). Subsequently, the cell was exposed to a transcellular current of  $1.7 \mu\text{A}$  for 8 min, and this treatment eliminated the fifth band (Fig. 8c).

The effect of transcellular current in our experiments (current  $1\text{--}3 \mu\text{A}$ , duration  $\leq 10$  min) was fully reversible. The location of bands susceptible to transcellular current differed for different cells. For example, in Figs. 7 and 8c the electric current eliminated the bands in the left cell part and in the middle of the cell, respectively. In experiments with passing electric current, a post-treatment effect became evident. When the current flow initiated band suppression, the band amplitude continued to decline for 10–15 min after switching the current off, prior to the band recovery.

We checked whether the combined application of low light and transcellular current would exert an additive action on the pH profile. For this purpose, the intensity range, where the pH profile markedly changes as a function of irradiance (Fig. 3a, curve 2) was chosen. We found that passing the transcellular current at low light ( $1.0 \mu\text{mol quanta m}^{-2} \text{s}^{-1}$ ) did not further reduce the number of bands, although it slightly suppressed the amplitude (cf. Fig. 8b and Fig. 8d). Thus, there is no simple additive effect of low light intensity and transcellular current.

## Discussion

This study has revealed characteristic modifications of pH pattern in *Chara* cells under changes in light intensity and during the transition from the homogenous state to the accomplished pH banding profile. The novel pH scanning method allows long-lasting measurements of

pH profiles with sufficient spatial resolution. Depending on cell and experimental conditions, the pH profiles for parallel lanes shifted along the cell perimeter were either similar (Fig. 4a and Fig. 4b) or strikingly different (Fig. 4c). What single-path pH profiles cannot show is that, for example, the alkaline peaks in curve 1 represent patches with some fine structure, rather than complete bands. The pH profiles 7–9 measured for equidistantly spaced lanes are almost flat, indicating that the pH heterogeneity is a localized phenomenon. At the same time, in other cells, the pH profiles were almost identical for all lanes, indicating a regular banding pattern (Fig. 4a and Fig. 4b). Some features of a single-path profile already contain hints on the type of pH heterogeneity: uniform peaks spaced by regular intervals are indicative of bands, whereas peaks of variable magnitude spaced by irregular intervals indicate the presence of a patchy pattern.

Our data show that, at low light levels, the pH pattern originates and durably exists in the form of spots or unclosed bands, whereas it evolves towards closed bands under light of high intensity and long exposures to light of moderate intensity. Under transition from dark to bright light, the rearrangement of spots to bands normally proceeds rather fast and cannot be precisely followed by pH scanning in multiple lanes, except for slowly responding cells. The use of low light intensities provides an opportunity to reproducibly detect the patch–band transitions, because the evolution of a banding profile is slowed down and incomplete. For example, pH profiles with one or a few bands are stable for hours at moderate light intensities, whereas the elevation of light intensity increases the number of bands and gives rise to multiphase pH profiles. Conversely, upon the transfer of a cell from darkness to bright light, alkaline bands are generated one by one during a relatively short period. It appears that



the transformation of pH profiles for a graded series of low-intensity regimes resembles the process of pattern formation at high light levels and that separate long-lived states attained in graded light of low intensity are similar to transient states rapidly emerging and ceasing in high light. Thus, studying the pH patterns at low light levels provides new insights into the process of pattern formation.

Several features of pH pattern modulation by light of graded intensities can be emphasized. Firstly, changes in light conditions in the low-intensity range affect the number rather than the stationary amplitude of bands. The intensity range where the band magnitude depends on light intensity is quite narrow, as can be seen from the sigmoid function with a steep transition from zero to full amplitude in Fig. 3b.

Secondly, upon cyclic exposures to decreasing and increasing light intensities, hysteresis occurs. When increasing the light intensity, the bands appeared at a significantly higher light level as compared to the intensities at which the last bands disappeared (Figs. 1, 2, 3). In fact, the descending branch of the  $\Delta\text{pH}$  versus light intensity plot could not be resolved for many cells; it occurred at such low light levels that accurate measurements of pH profiles were technically difficult. Only the adaptation of a cell to darkness finally removed the last pH bands. The hysteresis is also manifested by the existence of two stable states at the same light intensity of  $2.2 \mu\text{mol quanta m}^{-2} \text{s}^{-1}$ , either flat (upon increasing light) or with a well-developed banding pattern (upon decreasing light). In view of this bistable behavior connected with the abrupt generation of the alkaline bands upon a relatively small increment in light intensity, the pH band response is close to an all-or-none phenomenon.

Thirdly, the pH pattern generated at low light levels consisted of patches, and the transition to bright light was accompanied by patch–band rearrangement. Some alkaline spots were eliminated during this transition (Fig. 6). The newly arising alkaline bands are narrow, but they become broader during the evolution of pH pattern. During this process, some closely positioned peaks merge to a doublet. The changes associated with band formation include deletions, fusion, and widening of local peaks.

The transcellular current flow eliminated some bands in the pH profile without affecting the remaining bands. In this respect, the electric current effect was similar to the effect of lowering the light intensity. At the same time, these two effects were not additive. Elimination of some bands in the pH profile by low light level or the current flow was in marked contrast to the effect of other treatments (e.g., 5 mM  $\text{NH}_4\text{Cl}$  or 10 mM  $\text{KCl}$ ). These treatments caused a suppression of all peaks in the pH profile (Bulychev et al. 2001b). Our observation provides new evidence supporting the conclusion that light and electric current affect the same feedback regulatory system in cells of Characeae (Boels and Hansen 1982). It is also known that the electric field disturbs self-organization

patterns in physicochemical systems (Lobanov et al. 2000). The effect of the transcellular current seems mediated by a disturbance of local electric currents flowing inside the cell between acid and alkaline zones.

The aftereffect of the electric current is noteworthy and might reflect the gradual diffusion-mediated dissipation of the pH gradient when the process underlying its origin (operation of  $\text{H}^+$ -pump and/or functioning of high-pH channels) has been deactivated. However, considering the thickness  $\delta$  of unstirred layers in *Chara* as about 0.3 mm (Bulychev et al. 2001b), the time of post-treatment band inactivation (10–15 min) is too long for proton diffusion. It does not fit to the relation describing the diffusion time  $t_{1/2}$  in unstirred layers:  $t_{1/2} = 0.35\delta^2/D$ , where  $D \approx 10^{-4} \text{ cm}^2/\text{s}$  is the coefficient of proton diffusion. Thus, the aftereffect seems to reflect the modulation of pump or sink activity.

The results of the previous and our current study suggest that, after a stepwise illumination, the pH profiles undergo rearrangement from multiple patches to fewer regular bands. In our experiments, the locations of major alkaline peaks coincided with the previous ones, even when the spots were temporary and disappeared during the transition to the steady state (Fig. 6). The location of bands in the steady-state pH profile was also the same after reillumination as before dark adaptation. This is opposite to the inversion of the transmembrane current pattern after reillumination (Fisahn and Lucas 1990) observed on a particular group of *Nitella* cells, but is compatible with other data (Frost-Shartzer et al. 1992). It seems likely that the origin of primary heterogeneity in the pH distribution over the cell is distinct from the mechanisms underlying pattern evolution and resumption of band locations. The primary heterogeneity may arise from minute unbalances of photosynthetic activity in various parts of a chloroplast cylindrical layer; the possibility of alternative pathways of photosynthetic electron transport seems beneficial in this respect. On the other hand, the membrane–cytoplasmic interactions mediated by the cytoskeleton may be important for establishing cell polarity and organizing cell regions that are qualitatively different (Hollenbeck 2001). To find answers to these open questions is a challenge for further investigations.

**Acknowledgements** This work was supported by the Deutsche Forschungsgemeinschaft and the Russian Foundation for Basic Research (01-04-48075). We thank Dr. Wolfgang Jantoss for careful measurements of the spectral energy distribution of actinic light.

## References

- Beilby MJ, Mimura T, Shimmen T (1993) The proton pump, high pH channels, and excitation: voltage clamp studies of intact and perfused cells of *Nitellopsis obtusa*. *Protoplasma* 175:144–152
- Bisson MA, Walker NA (1980) The *Chara* plasmalemma at high pH. Electrical measurements show rapid specific passive uniport of  $\text{H}^+$  or  $\text{OH}^-$ . *J Membr Biol* 56:1–7

- Boels HD, Hansen UP (1982) Light and electrical current stimulate the same feedback system in *Nitella*. *Plant Cell Physiol* 23:343–346
- Bulychev AA, Cherkashin AA, Rubin AB, Vredenberg WJ, Zykov VS, Müller SC (2001a) Comparative study on photosynthetic activity of chloroplasts in acid and alkaline zones of *Chara corallina*. *Bioelectrochemistry* 53:225–232
- Bulychev AA, Polezhaev AA, Zykov SV, Plusnina TYu, Riznichenko GYu, Rubin AB, Jantoss W, Zykov VS, Müller SC (2001b) Light-triggered pH banding profile in *Chara* cells revealed with a scanning pH microprobe and its relation to self-organization phenomena. *J Theor Biol* 212:275–294
- Fisahn J, Lucas WJ (1990) Inversion of extracellular current and axial voltage profile in *Chara* and *Nitella*. *J Membr Biol* 113:23–30
- Fisahn J, Lucas WJ (1991) Autonomous local area control over membrane transport in *Chara* internodal cells. *Plant Physiol* 95:1138–1143
- Fisahn J, Hansen U-P, Lucas WJ (1992) Reaction kinetic model of a proposed plasma membrane two-cycle  $H^+$ -transport system of *Chara corallina*. *Proc Natl Acad Sci USA* 89:3261–3265
- Frost-Shartzner AA, Fisahn J, Lucas WJ (1992) Simultaneous measurement of extracellular current and membrane potential of *Chara corallina* internodal cells during light-induced modulation of  $H^+$  transport. *CR Acad Sci Paris Ser III* 315:247–254
- Hollenbeck P (2001) Cytoskeleton: microtubules get the signal. *Curr Biol* 11:820–823
- Lobanov AI, Plusnina TYu, Riznichenko GYu, Starozhilova TK, Rubin AB (2000) Effects of electric field on spatiotemporal patterning in the reaction–diffusion medium. *Biophysics* 45:483–489
- Lucas WJ (1975) The influence of light intensity on the activation and operation of the hydroxyl efflux system of *Chara corallina*. *J Exp Bot* 26:347–360
- Lucas WJ, Nuccitelli R (1980)  $HCO_3^-$  and  $OH^-$  transport across the plasmalemma of *Chara*: spatial resolution obtained using extracellular vibrating probe. *Planta* 150:120–131
- Lucas WJ, Ogata K (1985) Hydroxyl- and bicarbonate-associated transport processes in *Chara corallina*: studies on the light–dark regulation mechanism. *J Exp Bot* 36:1947–1958
- Lucas WJ, Keifer DW, Sanders D (1983) Bicarbonate transport in *Chara corallina*: evidence for cotransport of  $HCO_3^-$  with  $H^+$ . *J Membr Biol* 73:263–274
- Spear DG, Barr JK, Barr CE (1969) Localization of hydrogen ion and chloride fluxes in *Nitella*. *J Gen Physiol* 54:397–414
- Toko K, Chosa H, Yamafuji K (1985) Dissipative structures in the Characeae: spatial pattern of proton flux as a dissipative structure in Characean cells. *J Theor Biol* 114:127–175
- Toko K, Hayashi K, Yoshida T, Fujioshi T, Yamafuji K (1988) Oscillations of electric spatial pattern emerging from the homogenous state in Characean cells. *Eur Biophys J* 16:11–21
- Walker NA, Smith FA (1977) Circulating electric currents between acid and alkaline zones associated with  $HCO_3^-$  assimilation in *Chara*. *J Exp Bot* 28:1190–1206